Annals of Pharmacy Practice and Pharmacotherapy
ISSN: 3062-4436
2025, Volume 5, Issue 2, Page No: 98-110
Copyright CC BY-NC-SA 4.0
Available online at: www.galaxypub.co/page/journals

Galaxy Publication

Emergence of Hypervirulent and Multidrug-Resistant *Burkholderia cepacia* Complex Strains in Patients with COVID-19

Daniel Fischer[1]*, Laura Meier[1], Thomas Braun[2], Stefan Koch[2], Felix Roth[1]

[1]Department of Clinical Pharmacy and Drug Therapy, Faculty of Pharmacy, University of Freiburg, Freiburg, Germany.
[2]Department of Pharmacotherapy and Pharmaceutical Practice, Faculty of Medicine, Karlsruhe Institute of Technology, Karlsruhe, Germany.

***E-mail** ✉ daniel.fischer@outlook.com

Received: 29 June 2025; **Revised:** 10 October 2025; **Accepted:** 14 October 2025

ABSTRACT

Burkholderia species are opportunistic bacteria encountered in clinical settings, most frequently affecting individuals with cystic fibrosis. In our observations, members of the *Burkholderia cepacia* complex (Bcc) were also detected in patients with respiratory infections caused by viruses such as H7N9 influenza and SARS-CoV-2. Nevertheless, systematic investigation of Bcc co-infections with respiratory viruses remains limited. Accordingly, this study aimed to characterize COVID-19–Bcc and H7N9–Bcc co-infections by analyzing their genomic features, antimicrobial resistance profiles, and virulence-related traits. A retrospective study was conducted on 49 clinical isolates of the *Burkholderia cepacia* complex (Bcc) obtained from patients treated at a tertiary hospital in Zhejiang Province during outbreaks of H7N9 influenza and COVID-19. Among these isolates, 42 were recovered from H7N9 cases, while the remaining 7 were recovered from individuals infected with SARS-CoV-2. All isolates were subjected to antimicrobial susceptibility testing, virulence assessment using the *Galleria mellonella* larval infection model, and whole-genome sequencing to enable comprehensive molecular characterization of Bcc strains associated with COVID-19. Among the 49 Bcc strains tested, those recovered from COVID-19 patients accounted for 57.1% of all multidrug-resistant isolates. Analysis of median survival time in *G. mellonella* larvae revealed that COVID-19-associated Bcc strains killed the larvae more quickly and exhibited greater virulence compared to H7N9-associated Bcc ($P < 0.05$). Phylogenetic analysis suggested that COVID-19-related Bcc may have originated from H7N9-related Bcc through evolutionary changes. This study is the first to identify co-infection with *Burkholderia cepacia* complex (Bcc) in a substantial number of patients with respiratory tract infections, specifically those with H7N9 influenza and COVID-19. Our findings also suggest that Bcc strains associated with COVID-19 likely evolved from H7N9-linked Bcc and exhibit both enhanced virulence and multidrug resistance.

Keywords: Comparative genomic analysis, Hypervirulence, Multidrug-resistance, COVID-19, H7N9, *Burkholderia cepacia* complex

How to Cite This Article: Fischer D, Meier L, Braun T, Koch S, Roth F. Emergence of Hypervirulent and Multidrug-Resistant *Burkholderia cepacia* Complex Strains in Patients with COVID-19. Ann Pharm Pract Pharmacother. 2025;5(2):98-110. https://doi.org/10.51847/dYRmUkvueM

Introduction

The World Health Organization (WHO) has designated the novel coronavirus, “Severe Acute Respiratory Syndrome Coronavirus 2” (SARS-CoV-2), the causative agent of Coronavirus Disease 2019 (COVID-19), as one of the highly pathogenic β-coronaviruses capable of infecting humans, and it has sparked a worldwide pandemic [1]. The early clinical signs and transmission patterns of SARS-CoV-2 mirror those of influenza [2]. In a parallel manner, the outbreak stemming from human infection with avian influenza A (H7N9) virus has, much like SARS-CoV-2, resulted in substantial disease burden and exceptionally high fatality rates among humans [2]. It is well established, however, that respiratory viral infections markedly increase susceptibility to bacterial co-infections

© 2025 Annals of Pharmacy Practice and Pharmacotherapy

and superinfections [3]. Evidence indicates that bacterial co-infections occur in 20–30% of patients with severe influenza [4]. Such bacterial co-infections drive patients with viral illnesses to require greater medical resources and may give rise to more severe pathologies, ultimately heightening mortality rates [5].

Members of the genus Burkholderia are Gram-negative β-proteobacteria, abundantly present in aquatic environments, soil, and the rhizosphere of plants [6]. Possessing versatile metabolic capabilities and remarkable environmental resilience, Burkholderia can persist in hostile conditions and emerge as opportunistic pathogens within healthcare settings [4]. The foremost Burkholderia species implicated in human disease are *Burkholderia cepacia* complex (Bcc) and Burkholderia pseudomallei [7]. The Bcc group comprises *B. cepacia*, *Burkholderia multivorans*, and other species [8]. It predominantly afflicts individuals with cystic fibrosis and is considered a leading pathogen in clinical care, second only to the ESCAPE group [9]. Highly virulent Bcc strains have been responsible for outbreaks in multiple regions worldwide [10, 11]. Therapeutic management of these bacterial infections is exceedingly challenging owing to their pronounced antibiotic resistance profiles [12, 13]. Nevertheless, scant research has been conducted on the consequences of Bcc for patients already battling viral infections.

In hospital wards and intensive care units, co-infection with viruses and bacteria has been documented in up to 68% of cases, with profound effects on patient survival. Existing literature addressing SARS-CoV-2 and bacterial co-infection has largely centered on the identity and relative abundance of the infecting bacterial species. To date, however, investigations have not delved into the genetic makeup of these bacteria, their antimicrobial resistance patterns, virulence-associated traits, or their clinical impact on virally infected patients through a genomic lens [8]. In the current work, we identified SARS-CoV-2 and BCC co-infection in a subset of COVID-19 patients, a phenomenon also observed in individuals with H7N9. We therefore undertook a retrospective collection of BCC isolates from patients afflicted with H7N9 and COVID-19 at a tertiary hospital in Zhejiang Province spanning the years 2013 to 2020. This research categorized and compared the antimicrobial susceptibility, virulence phenotypes, and genomic attributes of recovered isolates, thereby uncovering the hypervirulent nature and multidrug resistance of BCC isolates from COVID-19 patients.

Materials and Methods

Sample collection and identification

A retrospective collection of 49 BCC isolates from individuals with H7N9 and COVID-19 at a tertiary hospital in Zhejiang Province spanning 2013 to 2020 was undertaken. Of these, 42 were recovered from H7N9 patients and seven from COVID-19 patients. To further control for natural bacterial evolutionary drift, Bcc strains cultured from other patients in 2020 were randomly selected as a comparator group. Every experimental strain originated from routine clinical laboratory workflows.

Conventional biochemical approaches yield questionable accuracy for the definitive identification of Bcc [8]. For this reason, matrix-assisted laser desorption/ionization time-of-flight mass spectrometry (MALDI-TOF/MS) (Bruker Daltonik GmbH, Bremen, Germany) was utilized for bacterial identification. In addition, high-throughput ANI analysis was performed on whole-genome sequencing data to achieve unambiguous species-level resolution within Bcc [14], with *B. cepacia* (GCF001718895) and B. multivorans (GCF000959525) serving as reference strains.

Antibiotic susceptibility testing

Minimum inhibitory concentrations (MICs) for the tested antibiotics (Dalian Meilun Biotech Co., Ltd., Dalian, China) were determined by the agar dilution method [15]. The antibiotic panel consisted of meropenem, ceftazidime, minocycline, levofloxacin, trimethoprim-sulfamethoxazole, and chloramphenicol. Result interpretation followed the breakpoints established by the Clinical and Laboratory Standards Institute (CLSI) (https://clsi.org). Escherichia coli ATCC 25922 and Pseudomonas aeruginosa ATCC 27853 served as the quality control organisms.

Survival rates of galleria mellonella larvae challenged with Bcc

BCC colonies were plated on blood agar and left to multiply overnight at 37°C in a temperature-controlled incubator. The resulting growth was harvested and resuspended in NaCl solution until the optical density reached 1.0 at 600 nm. Groups containing ten *G. mellonella*, each at an approximate body mass of 250 mg, were formed

through random assignment. Into every larva, a 20μL inoculum of 1×10^7 CFU/mL bacterial suspension was delivered by injection. The untreated control arm received only sterile PBS. Incubation of all larvae was carried out at 37°C, with their condition observed at 12-hour intervals throughout the 7-day incubation period [16]. The study used *E. coli* ATCC 25922 for quality assurance.

Biofilm quantification

Broth cultures in Luria-Bertani medium (LB, Sangon Biotech, China) were grown overnight, after which cells were pelleted, washed, and diluted in LB to a target OD_{600} of 0.1. From each adjusted suspension, a 200 μL portion was transferred to individual wells of a 96-well polystyrene microplate (Corning). Triplicate technical replicates were prepared for each specimen, and incubation was performed at 37 °C for 24 h. Subsequent processing involved three washes with PBS (0.1 mol/L, pH 7.4), the addition of 100 μL of 0.1% crystal violet, and a 15-minute incubation step at ambient conditions. Upon another round of triple PBS rinses, 200 μL of isopropanol was introduced to each well. Gentle mixing was performed before absorbance measurement at OD_{600} [16].

growth assay

Using Mueller-Hinton broth (MHB) medium (Cat. No. CM0405; OXOID, UK), BCC strains were first enriched overnight, then diluted to an OD_{600} value of 0.02 (corresponding to roughly 1×10^5 CFU/mL) in fresh medium and further cultivated at 37 °C for 18 h with strong rotary shaking (220 rpm). To begin the assay, 180 μL of MHB was preloaded into 96-well polystyrene microplates, to which 20 μL of the standardized bacterial suspension was added. At hourly time points, cell density was quantified by monitoring the OD_{600} [16]. The observation window lasted continuously for over 40 h.

Whole-genome sequencing (WGS) and data analysis

An OMEGA Bacterial DNA Kit (Omega Bio-tek, Norcross, GA, USA) was used to purify genomic DNA from the isolates. Whole-genome sequencing was executed on the Illumina NovaSeq 6000-PE150 system (Illumina, San Diego, CA, USA). The raw sequencing reads were assembled de novo into contiguous genome sequences using SPAdes 3.11. Existing web-based pipelines were exploited to annotate antimicrobial resistance determinants (http://www.genomicepidemiology.org/), virulence-associated genes (http://www.mgc.ac.cn/VFs/), and sequence types through MLST analysis (http://pubmlst.org/).

Phylogenetic reconstruction and analysis

Using the genome of B. multivorans (GCF_000959525.1) as a reference scaffold [17], the GATK toolkit (GATK (broadinstitute.org)) pinpointed single-nucleotide polymorphisms. Gubbins version 2.4.1 subsequently removed putative recombination hotspots identified by unusually dense clusters of base changes [18]. A maximum-likelihood phylogenetic reconstruction was then inferred from the filtered core-genome alignment using FastTree with the GTR+CAT substitution model [19]. The software PHYLOViZ 2.0 (http://www.phyloviz.net/tutorials.html) facilitated the construction of a minimum spanning tree derived from core-genome SNPs [20]. To place the 49 Bcc strains from this work in a broader context, comparisons were drawn with publicly deposited records in NCBI. A core SNP set obtained using kSNP [21] was used to construct a maximum-likelihood tree, which was displayed in iTOL (https://itol.embl.de/). Screening of the CARD repository (https://card.mcmaster.ca/) permitted examination of the complement of efflux pump genes carried by each isolate.

Statistical analysis

The genome-wide association study (GWAS) methodology was applied in RStudio. Group-wise statistical comparisons across the three datasets used the Kruskal–Wallis rank-sum test. A significance cutoff was fixed at a P-value of 0.05; any P falling below 0.05 constituted a statistically significant difference.

Data availability

The assembled whole-genome datasets for all 49 Bcc strains have been made publicly available through GenBank under the consecutive accession numbers JAGXEV000000000 to JAGXCZ000000000.

Results and Discussion

Identification result of Bcc

The study enrolled patients with H7N9 influenza treated in a tertiary hospital in Zhejiang Province during 2013–2014, as well as patients with COVID-19 admitted between 2019 and 2020. From these cases, 49 *B. cepacia* complex (Bcc) isolates were recovered, including 42 from H7N9 infections and 7 from COVID-19 cases.

Combined identification using MALDI-TOF MS and average nucleotide identity (ANI) analysis classified the isolates into 21 *B. multivorans* and 28 *B. cepacia* strains **(Figure 1).**

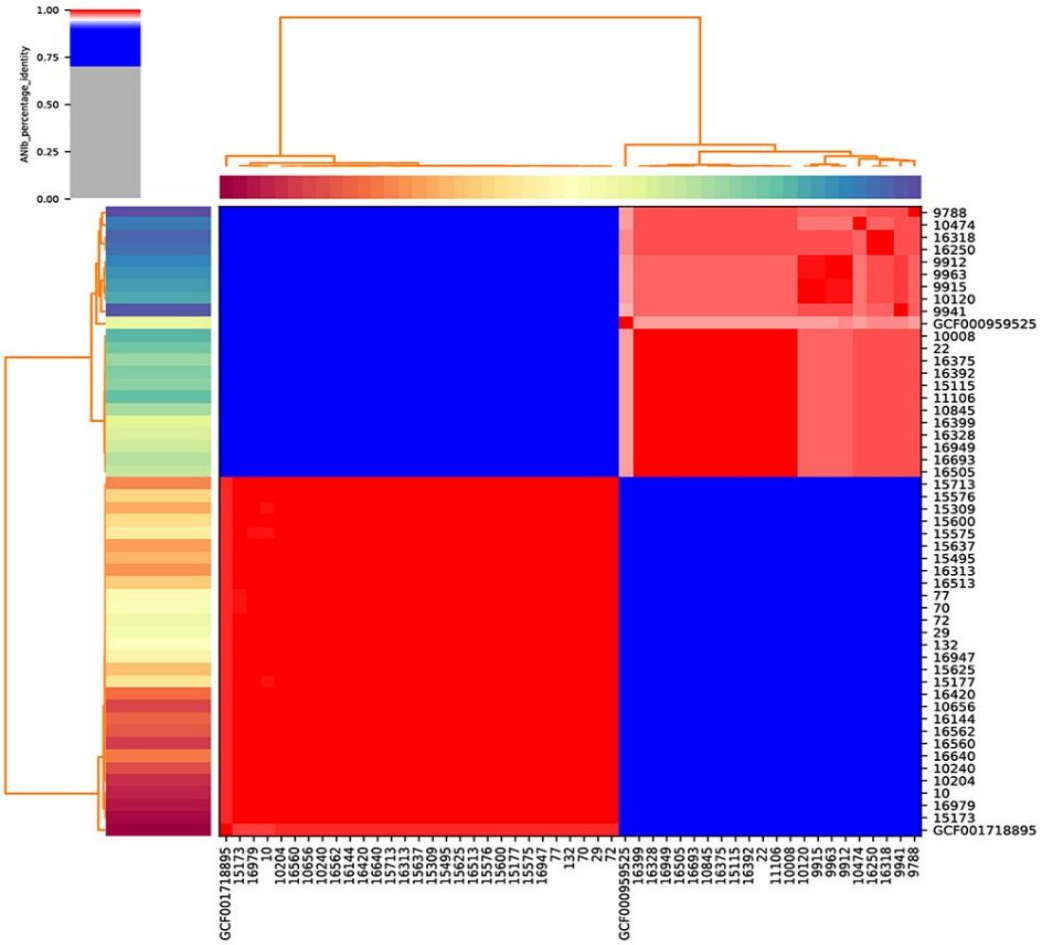

Figure 1. The ANI-based taxonomic assignment of the 49 *Bcc* isolates. Genome comparisons were performed against *B. cepacia* (GCF001718895) and *B. multivorans* (GCF000959525) as reference strains to determine species identity. In the visualization, isolates clustering with *B. cepacia* are highlighted in red on the horizontal axis, whereas those aligning with *B. multivorans* are shown in blue.

Molecular characteristics of 14 BCC

Figure 2 summarizes the distribution of antimicrobial resistance determinants identified in the study isolates. Aminoglycoside resistance genes were assessed only in two *B. multivorans* strains. Virulence-associated loci identified in the Bcc genomes included genes involved in flagellar assembly, chemotaxis systems, type IV pili, N-acyl homoserine lactone–mediated regulation, and capsular polysaccharide biosynthesis.

Multilocus sequence typing (MLST) results are also presented in **Figure 2.** No corresponding sequence types were identified for *B. cepacia*, whereas ST1008 was the predominant type among *B. multivorans* isolates (57.1%). Other detected sequence types within *B. multivorans* included ST274 (4.8%), ST618 (4.8%), ST16 (9.5%), ST616 (9.5%), and ST749 (9.5%).

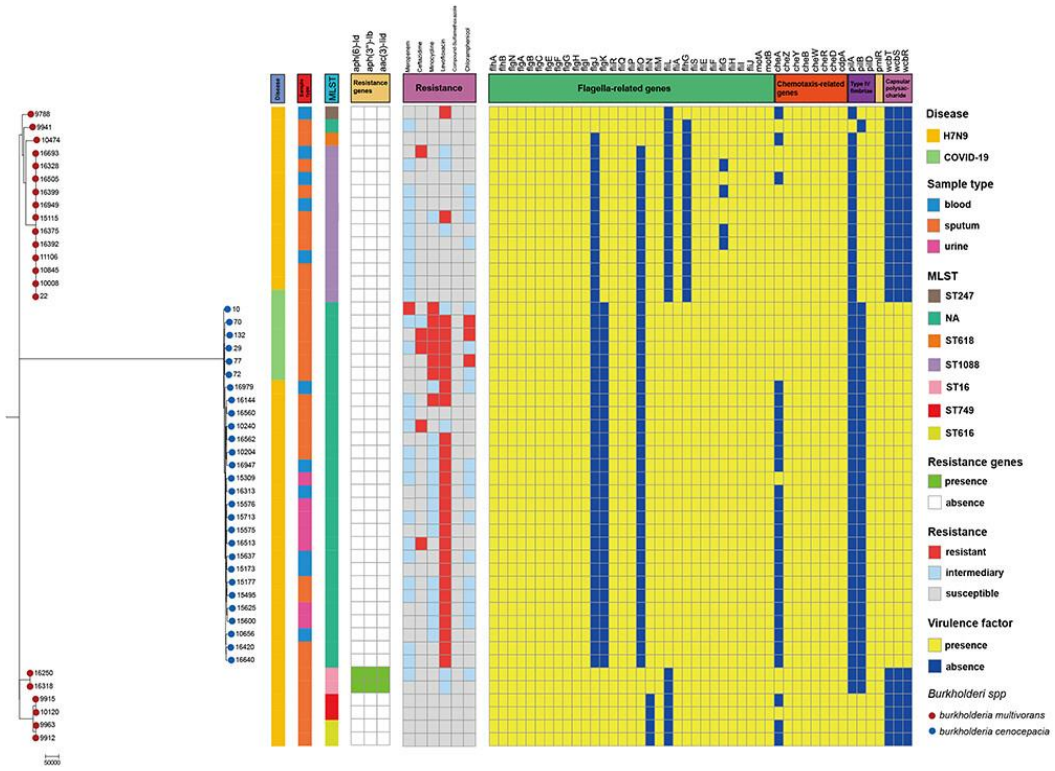

Figure 2. The phylogenetic reconstruction of *B. cepacia* and *B. multivorans* isolates. The tree integrates multiple layers of annotation, including isolate origin, MLST profiles, antimicrobial resistance gene content, phenotypic susceptibility results, and virulence gene distributions.

Antibiotic resistance profiles of 49 BCC

Antimicrobial susceptibility results are summarized in **Figure 2.** In isolates from H7N9 patients, resistance rates were 0% for meropenem, 7% for ceftazidime, 2.3% for minocycline, 52.4% for levofloxacin, and 0% for both trimethoprim–sulfamethoxazole and chloramphenicol. In contrast, COVID-19–associated isolates showed higher resistance rates, including 14.3% for meropenem, 28.6% for ceftazidime, 85.7% for minocycline, 71.4% for levofloxacin, 0% for trimethoprim–sulfamethoxazole, and 42.9% for chloramphenicol.

Overall, no multidrug-resistant (MDR) strains were detected among H7N9-derived isolates, whereas 57.1% of COVID-19–derived isolates were classified as MDR.

Among the 30 reference isolates, resistance to levofloxacin reached 70%, while no resistance was observed for minocycline or trimethoprim–sulfamethoxazole. Only three isolates in this reference group were identified as MDR strains.

Growth kinetics

To evaluate potential differences in in vitro proliferation, growth curves of the *Bcc* isolates were assessed in Mueller–Hinton broth at 37 °C **(Figure 3).** Doubling times were calculated and compared between groups. Statistical analysis showed no significant difference in growth kinetics between the two sets of isolates (P = 0.16).

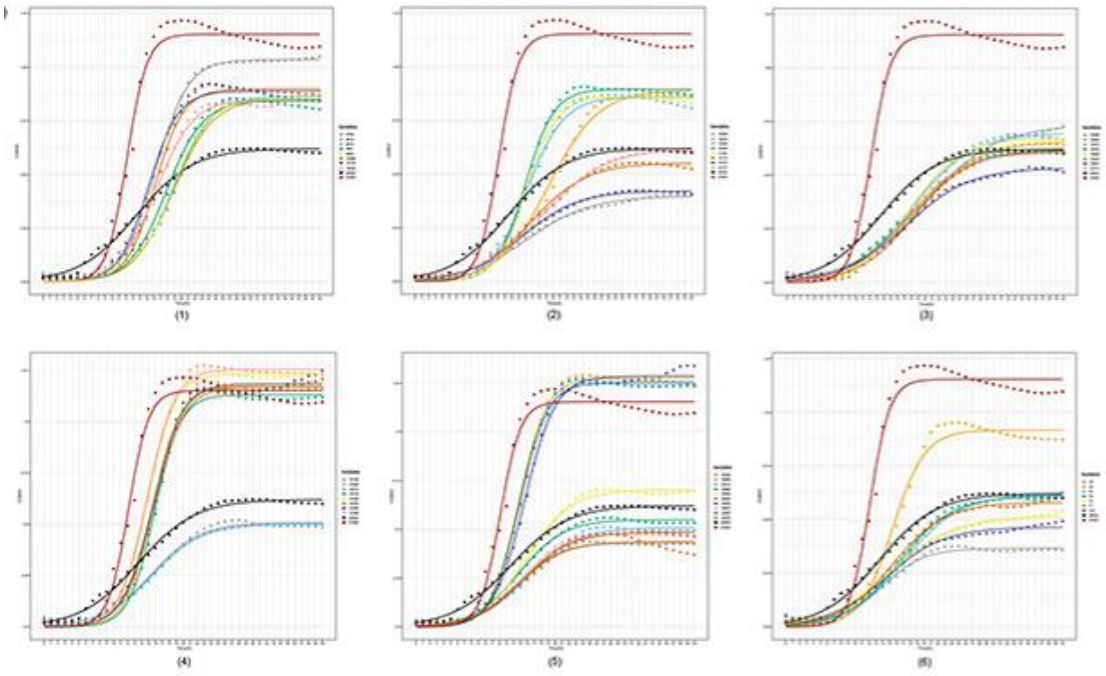

a)

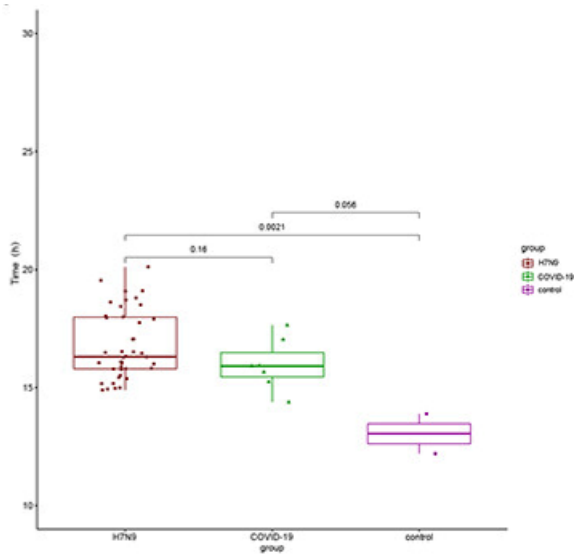

b)

Figure 3. The in vitro growth dynamics of *B. cepacia* and *B. multivorans* isolates. Panel (a) presents the growth curves, where plots (1)–(5) correspond to H7N9-associated Bcc isolates and plot (6) represents COVID-19–associated Bcc isolates. Panel (b) compares growth parameters between H7N9-Bcc, COVID-19-Bcc, and the control group; statistical significance was defined as $P < 0.05$.

G. mellonella infection model

In vivo virulence was evaluated using the *Galleria mellonella* infection model. Median survival time of larvae infected with H7N9- and COVID-19-associated Bcc isolates was compared to assess differences in pathogenic potential **(Figure 4).** Statistical analysis demonstrated that larvae infected with COVID-19-derived Bcc exhibited a significantly shorter median survival time, indicating higher virulence ($P = 0.00041$).

Furthermore, when compared with 30 reference isolates, COVID-19-associated Bcc strains again showed a markedly reduced larval survival time, consistent with enhanced virulence relative to the reference group ($P = 0.00041$).

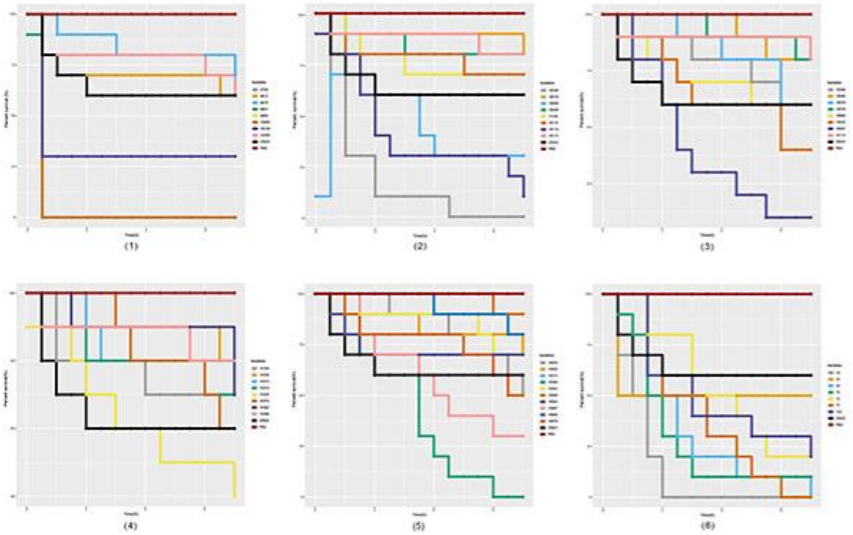

a)

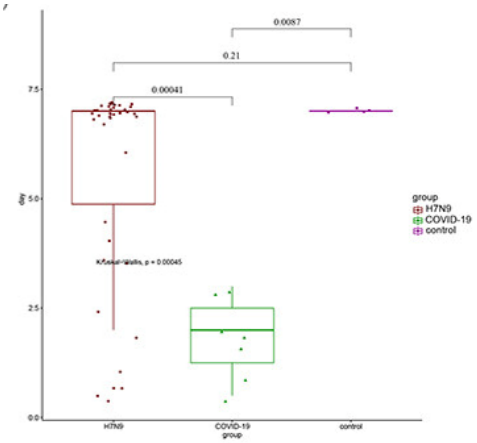

b)

Figure 4. In vivo pathogenicity of Bcc isolates in the *Galleria mellonella* model. Panel (a) shows larval survival following infection with individual strains: sets (1–5) correspond to isolates from H7N9 cases, while set (6) represents isolates from COVID-19 patients. Panel (b) presents a comparative analysis of survival outcomes across the H7N9, COVID-19, and control groups, with statistical significance set at $P < 0.05$.

Comparison of biofilm formation ability

Biofilm formation represents a major clinical concern in hospital environments, particularly in intensive care settings and among immunocompromised individuals. Therefore, we evaluated and compared the biofilm-forming capacity of *Bcc* isolates derived from H7N9 and COVID-19 patients [22].

Following crystal violet staining, biofilms were solubilized with isopropanol and quantified by measuring absorbance at 600 nm (OD600). Statistical comparison between the two groups revealed no significant difference in biofilm production ($P = 0.084$). The corresponding results are presented in **Figure 5.**

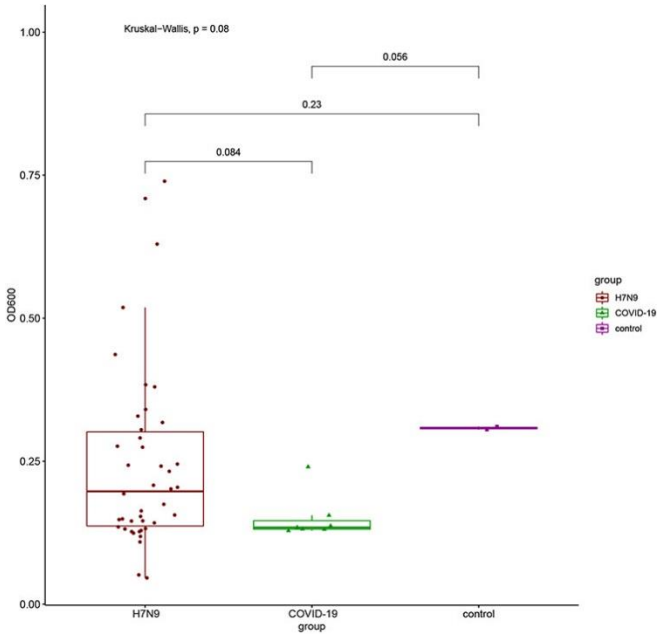

Figure 5. The assessment of biofilm production in *B. cepacia* and *B. multivorans* isolates. Biofilm levels were compared across strains originating from H7N9 patients, COVID-19 patients, and the control group, with $P < 0.05$ considered statistically significant.

Phylogeny analysis

A SNP-based phylogenetic reconstruction was performed to explore the genetic relationships among isolates. The resulting tree separated *B. cepacia* and *B. multivorans* into distinct clades, with strains of identical ST types clustering together. In *B. cepacia*, the isolate recovered from a COVID-19 patient formed an independent branch, whereas isolates from the same patient and sample type clustered together **(Figure 2).**

To further investigate the broader evolutionary context and potential ecological origins, a kSNP3-based phylogenetic analysis was conducted. Publicly available genomes from NCBI (year 2000 onwards) were included alongside the 49 study isolates. For *B. multivorans*, 156 clinical isolates (88.1%) and 21 environmental isolates (11.9%) were identified. For *B. cepacia*, 50 clinical isolates were included, with clinical strains comprising 88.1% of the dataset, including the 28 *B. cepacia* isolates from this study **(Figure 6).**

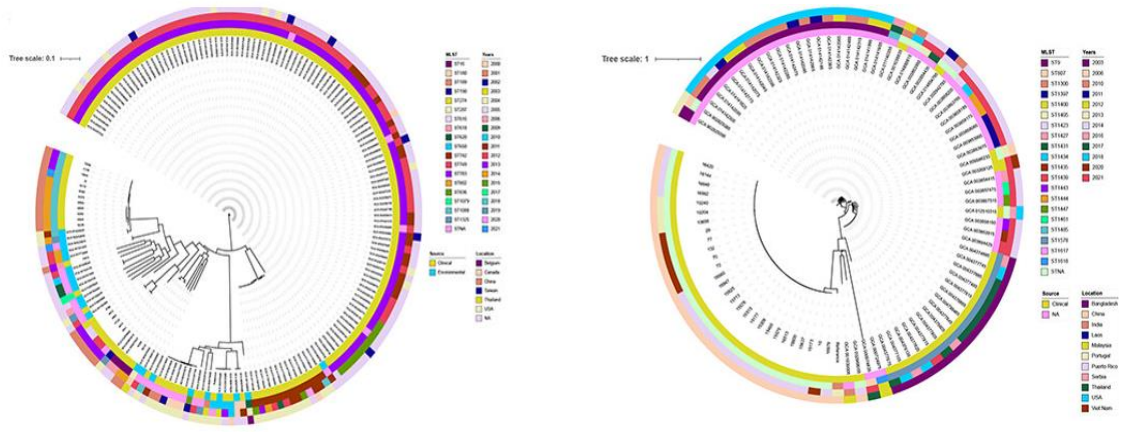

a) b)

Figure 6. The phylogenetic relationships of global *Bcc* isolates. Panel (a) shows the phylogeny of 177 *B. multivorans* strains, with concentric annotation rings indicating, from inner to outer layers, sample source, sequence type (ST), year of isolation, and geographic origin. Panel (b) displays a similar analysis of 92 B. cepacia isolates, with the same metadata arranged in sequential outer rings.

Concurrent viral and bacterial infections persistently endanger the lives of affected patients. Nevertheless, research has yet to examine the bacteria's genetic makeup, antimicrobial resistance patterns, virulence characteristics, or the clinical consequences of viral illnesses through a genomic lens. Our retrospective review uncovered co-occurrence of SARS-CoV-2 and BCC in individuals diagnosed with COVID-19, and a similar phenomenon was observed in H7N9 cases. Motivated by this, the present study retrospectively gathered 49 isolates from Bcc co-infected COVID-19 and H7N9 patients, employing whole-genome sequencing for the first time to establish that COVID-19-Bcc appears to have descended from H7N9-Bcc and possesses hypervirulent and multidrug-resistant traits. Six antibiotics listed by CLSI were selected for BCC resistance profiling. The data indicated that resistance frequencies in COVID-19-Bcc were higher than those in H7N9-Bcc. Levofloxacin exhibited the highest resistance rate among H7N9-Bcc (52.4%), while other agents ranged from 0% to 7%. Among COVID-19-Bcc, the antibiotics with the peak resistance rates were minocycline and levofloxacin (85.7% and 71.4%, respectively). The percentage of strains displaying multidrug resistance was 57.1% in COVID-19-Bcc versus 0% in H7N9-Bcc, highlighting the multidrug resistance of COVID-19-Bcc [23]. Both cohorts remained fully susceptible to trimethoprim-sulfamethoxazole (0% resistance), confirming its reliable efficacy against Bcc infections [24].

B. multivorans and *B. cepacia*, members of the genus Burkholderia, stand as notable pathogens. The marked antibiotic resistance of Bcc makes the infections it causes particularly challenging to treat [25]. Of the 49 Bcc isolates, merely two B. multivorans strains harbored quinolone resistance genes. Both isolates—16250 and 16318, carrying resistance determinants—originated from a 62-year-old female H7N9 patient. No resistance genes were identified in the other 47 BCC strains. The mechanistic basis of antibiotic resistance in BCC has been extensively investigated, revealing efflux pump overexpression as the principal driver. Consistent with other non-enteric Gram-negative bacteria, pumps of the resistance nodulation cell division (RND) family represent the predominant efflux systems operational in Bcc [26]. Upregulation of these pumps can confer upon bacteria the ability to withstand diverse antibiotic classes, including glycosides, chloramphenicol, fluoroquinolones, and tetracyclines [18].

As an opportunistic pathogen, BCC can sustain chronic respiratory tract infections in cystic fibrosis patients, posing significant obstacles to effective clinical management [18]. A substantial number of Burkholderia species harbor considerable pathogenic potential [25, 27]. In this work, we leveraged the *G. mellonella* larva infection model to compare the virulence capacities of COVID-19-Bcc and H7N9-Bcc. This model has been broadly adopted to evaluate virulence across numerous bacterial species and is frequently applied in Burkholderia-focused investigations [20]. As illustrated in **Figure 3,** the median lethal time for COVID-19-Bcc proved shorter than that for H7N9-Bcc, reflecting the greater virulence of the former. The pathogenicity of bacteria is largely determined by invasive enzymes, adhesins, and secretion systems. Colonization with hypervirulent strains leaves patients more vulnerable to invasive disease, deteriorates their clinical condition, and greatly complicates therapeutic efforts [28]. Bcc organisms can construct biofilms on non-living surfaces (such as glass and plastic) as well as living surfaces (such as epithelial cells), and these structures are instrumental in perpetuating persistent infection [29]. Biofilm formation is intimately linked to bacterial virulence [30], as it facilitates colonization across diverse environments and protects the microbial community from harmful host factors such as lysozyme and complement proteins [31]. The biofilm-forming capacity did not differ significantly between COVID-19-Bcc and H7N9-Bcc **(Figure 4).** Moreover, comparison of growth kinetics revealed no significant difference between the two groups **(Figure 5).** Thus, while COVID-19-Bcc demonstrates elevated virulence, biofilm production and growth velocity remain unaltered. We accordingly compared the virulence gene repertoires of COVID-19-Bcc and H7N9-Bcc to provide evidence supporting the virulence enhancement of COVID-19-Bcc.

Exceptionally virulent and transmissible Bcc lineages can cause outbreaks of clinical infection [32]. In the current analysis, we detected multiple genes associated with virulence, capsular polysaccharide synthesis, N-acyl homoserine lactone-dependent quorum sensing, Type IV pili (Tfp), chemotaxis, and flagellar biogenesis. Pili (fimbriae) expressed on the bacterial cell surface participate in pathogenesis primarily through attachment to host cells. In BCC, the cable pilus gene (Cbl) is the variant commonly reported [33]; however, the genes detected in this study were pilA, pilB, and pilD. These three genes, which encode essential virulence factors within the Tfp system, have been thoroughly characterized across a range of Gram-negative pathogens [34]. Flagellin, the exclusive known ligand for Toll-like receptor 5 (TLR5), can amplify inflammatory responses and precipitate lung damage [35, 36]. Capsular polysaccharide is a crucial virulence determinant that enables bacteria to circumvent or neutralize host immune defenses [16]. It is noteworthy that statistical analyses identified the chemotaxis gene

CheA as a potential contributor to the virulence divergence between COVID-19-Bcc and H7N9-Bcc ($P < 0.05$). The signal transduction and response regulation framework governing chemotaxis has been rigorously detailed in *Escherichia coli* [37]. Upon environmental stimulation, membrane-bound receptors drive autophosphorylation of the cytoplasmic histidine autokinase CheA, which assembles into a complex with the receptor via the coupling protein CheW. CheA subsequently transfers its phosphate moiety to CheY, enabling CheY to engage the flagellar motor and switch its rotational direction [38]. Earlier studies have demonstrated that intact chemotaxis and its associated regulatory cascade are prerequisites for full bacterial virulence [39]. During propagation in human serum, genes encoding the machinery required for chemotaxis and motility become upregulated, suggesting these functions may play a prominent role during bloodstream infection [40].

To reconstruct the evolutionary trajectory of the 49 Bcc isolates and pinpoint possible ancestral reservoirs and geographic origins, phylogenetic inference was carried out using kSNP3. All *B. multivorans* and *B. cepacia* genomes deposited in the NCBI database from 2000 onward were incorporated into the phylogenetic analysis. Core-genome phylogenetics encompassed 177 B. multivorans and 92 *B. cepacia* strains. Examination of *B. multivorans* indicated that clinical specimens constituted the predominant source of the isolates. As illustrated in **Figure 6**, the ST1088 B. multivorans strains from this investigation clustered in a shared clade with ST1325, and GCA_001529925 originating from the USA fell within the same subclade as the ST1088 B. multivorans characterized here. GCA_001529925 was recovered from an environmental sample collected in the USA in 2011. The phylogenetic findings allow us to deduce a plausible evolutionary origin for the ST1088 B. multivorans described in this work. Given the considerable geographic separation between the ST1088 B. multivorans and ST1088 GCA_001529925, independent evolutionary paths appear likely. Assessment of *B. cepacia* uncovered 50 clinical isolates, representing 88.1% of the total, among which were 28 strains of *B. cepacia* from the present study. Excluding strains lacking precise ST designations, the most prevalent sequence type worldwide was ST9 (21.7%), followed by ST1578 (16.3%). The isolates displaying the closest relatedness to the *B. cepacia* strains in this study were reference genomes from China. These reference strains originated in Jiujiang City, China, and were isolated from lake water samples. Although the *B. cepacia* strains analyzed here were collected across different years, all exhibited a high degree of genetic homogeneity when benchmarked against NCBI entries. The phylogenetic outcomes suggest that COVID-19-Bcc likely descended from H7N9-Bcc. That said, the literature on Burkholderia lags considerably behind that on ESKAPE pathogens. Consequently, a detailed dissection of its origins and pathogenic mechanisms remains out of reach, underscoring the imperative to bolster surveillance and investigation of this bacterial group.

Notwithstanding the relatively well-characterized phenotype of the hypervirulent and multidrug-resistant COVID-19-Bcc strains, the mechanistic underpinnings driving this phenomenon remain obscure. We postulate two potential explanations: first, infection with the novel coronavirus may compromise host immune function [41, 42], and this state of immunosuppression could remodel the host's internal milieu, thereby facilitating colonization by highly virulent and resistant strains; second, a substantial proportion of individuals infected with the novel coronavirus concurrently develop serious bacterial infections, and the pervasive administration of antibiotics may have acted as a dominant selective force steering strain evolution toward hypervirulence and multidrug resistance [43]. Moreover, hypervirulent and drug-resistant strains may propagate within hospital settings via environmental contamination, medical apparatus, and the horizontal dissemination of resistance determinants, presenting a grave menace to public health. Devising strategies to confront this challenge thus constitutes a matter of considerable urgency.

While the development of novel antibiotics targeting emerging bacterial targets remains an important pursuit, the judicious deployment of existing antimicrobials is even more vital [44, 45]. This entails rigorously curtailing antibiotic use, avoiding unwarranted prescriptions, and ensuring that the appropriate agent and dosage are administered when a genuine clinical need arises [46]. Healthcare facilities ought to enforce rigorous infection prevention and control protocols, encompassing hand hygiene, isolation of affected patients, routine decontamination of medical devices and the surrounding environment, and systematic monitoring of resistance trends. The synergistic application of these measures can effectively slow the spread of resistance, preserve antibiotic potency, and provide a defense against future resistant strains.

Conclusion

Through comparative analysis of 49 Bcc strains obtained from patients co-infected with COVID-19 and H7N9, it was established that COVID-19-Bcc probably evolved from H7N9-Bcc and that COVID-19-Bcc isolates exhibit multidrug resistance and heightened virulence relative to H7N9-Bcc isolates, indicating that enhanced detection and dedicated research on this bacterial group are warranted.

Acknowledgments: The authors would like to express their gratitude to all participants, study coordinators, and administrative staff for their valuable support throughout the research. All authors were involved in data analysis, manuscript preparation and revision, approval of the final version for publication, and take full responsibility for the integrity of the work.

Conflict of Interest: None

Financial Support: The study was financially supported by grants from the National Key R&D Program of China (2016YFD0501105, 2017YFC1200203) and the National Natural Science Foundation of China (82072314).

Ethics Statement: This study was performed in accordance with the principles of the Declaration of Helsinki and received ethical approval from the Institutional Review Board of The First Affiliated Hospital of Zhejiang University (approval No. 2021IIT372). Given the retrospective design and the use of anonymized data, the ethics committee waived the requirement for informed consent. All data were managed under strict confidentiality to protect patient privacy.

References

1. Noureddine FY, Chakkour M, El Roz A, Reda J, Al Sahily R, Assi A, et al. The emergence of SARS-CoV-2 variant(s) and its impact on the prevalence of COVID-19 cases in the Nabatieh Region, Lebanon. Med Sci. 2021;9(2):40.
2. Zou L, Ruan F, Huang M, Liang L, Huang H, Hong Z, et al. SARS-CoV-2 viral load in upper respiratory specimens of infected patients. N Engl J Med. 2020;382(12):1177-9.
3. Bengoechea JA, Bamford CG. SARS-CoV-2, bacterial co-infections, and AMR: the deadly trio in COVID-19? EMBO Mol Med. 2020;12(7):e12560.
4. Rice TW, Rubinson L, Uyeki TM, Vaughn FL, John BB, Miller RR 3rd, et al. Critical illness from 2009 pandemic influenza A virus and bacterial co-infection in the United States. Crit Care Med. 2012;40(5):1487-98.
5. Martin-Loeches I, Sanchez-Corral A, Diaz E, Granada RM, Zaragoza R, Villavicencio C, et al. Community-acquired respiratory co-infection in critically ill patients with pandemic 2009 influenza A(H1N1) virus. Chest. 2011;139(3):555-62.
6. Eberl L, Vandamme P. Members of the genus Burkholderia: good and bad guys. F1000Res. 2016;5:1007.
7. Schaefers MM. Regulation of virulence by two-component systems in pathogenic Burkholderia. Infect Immun. 2020;88(7).
8. Devanga Ragupathi NK, Veeraraghavan B. Accurate identification and epidemiological characterization of Burkholderia cepacia complex: an update. Ann Clin Microbiol Antimicrob. 2019;18(1):7.
9. Henry DA, Mahenthiralingam E, Vandamme P, Coenye T, Speert DP. Phenotypic methods for determining genomovar status of the Burkholderia cepacia complex. J Clin Microbiol. 2001;39(3):1073-8.
10. Biddick R, Spilker T, Martin A, LiPuma JJ. Evidence of transmission of Burkholderia cepacia, Burkholderia multivorans and Burkholderia dolosa among persons with cystic fibrosis. FEMS Microbiol Lett. 2003;228(1):57-62.
11. Mahenthiralingam E, Urban TA, Goldberg JB. The multifarious, multireplicon Burkholderia cepacia complex. Nat Rev Microbiol. 2005;3(2):144-56.
12. Dance D. Treatment and prophylaxis of melioidosis. Int J Antimicrob Agents. 2014;43(4):310-8.
13. Podnecky NL, Rhodes KA, Mima T, Drew HR, Chirakul S, Wuthiekanun V, et al. Mechanisms of resistance to folate pathway inhibitors in Burkholderia pseudomallei: deviation from the norm. mBio. 2017;8(5).
14. Jain C, Rodriguez RL, Phillippy AM, Konstantinidis KT, Aluru S. High throughput ANI analysis of 90K prokaryotic genomes reveals clear species boundaries. Nat Commun. 2018;9(1):5114.

15. Xu H, Wang X, Yu X, Zhang Y, Li A, Yang X, et al. First detection and genomics analysis of KPC-2-producing Citrobacter isolates from river sediments. Environ Pollut. 2018;235:931-7.
16. Niu T, Guo L, Luo Q, Zhou K, Yu W, Chen Y, et al. Wza gene knockout decreases Acinetobacter baumannii virulence and affects Wzy-dependent capsular polysaccharide synthesis. Virulence. 2020;11(1):1-13.
17. Johnson SL, Bishop-Lilly KA, Ladner JT, Daligault HE, Davenport KW, Jaissle J, et al. Complete genome sequences for 59 Burkholderia isolates, both pathogenic and near neighbor. Genome Announc. 2015;3(2):e00159-15.
18. Croucher NJ, Page AJ, Connor TR, Delaney AJ, Keane JA, Bentley SD, et al. Rapid phylogenetic analysis of large samples of recombinant bacterial whole genome sequences using Gubbins. Nucleic Acids Res. 2015;43(3):e15.
19. Price MN, Dehal PS, Arkin AP. FastTree: computing large minimum evolution trees with profiles instead of a distance matrix. Mol Biol Evol. 2009;26(7):1641-50.
20. Lieberman TD, Michel JB, Aingaran M, Potter-Bynoe G, Roux D, Davis MR Jr, et al. Parallel bacterial evolution within multiple patients identifies candidate pathogenicity genes. Nat Genet. 2011;43(12):1275-80.
21. Gardner SN, Slezak T, Hall BG. kSNP3.0: SNP detection and phylogenetic analysis of genomes without genome alignment or reference genome. Bioinformatics. 2015;31(17):2877-8.
22. Lesouhaitier O, Clamens T, Rosay T, Desriac F, Louis M, Rodrigues S, et al. Host peptidic hormones affecting bacterial biofilm formation and virulence. J Innate Immun. 2019;11(3):227-41.
23. Magiorakos AP, Srinivasan A, Carey RB, Carmeli Y, Falagas ME, Giske CG, et al. Multidrug-resistant, extensively drug-resistant and pandrug-resistant bacteria: an international expert proposal for interim standard definitions for acquired resistance. Clin Microbiol Infect. 2012;18(3):268-81.
24. Nimri L, Sulaiman M, Hani OB. Community-acquired urinary tract infections caused by Burkholderia cepacia complex in patients with no underlying risk factor. JMM Case Rep. 2017;4(1):e005081.
25. Podnecky NL, Rhodes KA, Schweizer HP. Efflux pump-mediated drug resistance in Burkholderia. Front Microbiol. 2015;6:305.
26. Guglierame P, Pasca MR, De Rossi E, Buroni S, Arrigo P, Manina G, et al. Efflux pump genes of the resistance-nodulation-division family in Burkholderia cenocepacia genome. BMC Microbiol. 2006;6:66.
27. Saldias MS, Valvano MA. Interactions of Burkholderia cenocepacia and other Burkholderia cepacia complex bacteria with epithelial and phagocytic cells. Microbiology. 2009;155(Pt 9):2809-17.
28. Holden MT, Feil EJ, Lindsay JA, Peacock SJ, Day NP, Enright MC, et al. Complete genomes of two clinical Staphylococcus aureus strains: evidence for the rapid evolution of virulence and drug resistance. Proc Natl Acad Sci U S A. 2004;101(26):9786-91.
29. Coenye T. Social interactions in the Burkholderia cepacia complex: biofilms and quorum sensing. Future Microbiol. 2010;5(7):1087-99.
30. Suppiger A, Schmid N, Aguilar C, Pessi G, Eberl L. Two quorum sensing systems control biofilm formation and virulence in members of the Burkholderia cepacia complex. Virulence. 2013;4(5):400-9.
31. Ganesh PS, Vishnupriya S, Vadivelu J, Mariappan V, Vellasamy KM, Shankar EM. Intracellular survival and innate immune evasion of Burkholderia cepacia: improved understanding of quorum sensing-controlled virulence factors, biofilm, and inhibitors. Microbiol Immunol. 2020;64(2):87-98.
32. Sousa SA, Feliciano JR, Pita T, Guerreiro SI, Leitão JH. Burkholderia cepacia complex regulation of virulence gene expression: a review. Genes (Basel). 2017;8(1):43.
33. Sun L, Jiang RZ, Steinbach S, Holmes A, Campanelli C, Forstner J, et al. The emergence of a highly transmissible lineage of cbl+ Pseudomonas (Burkholderia) cepacia causing CF centre epidemics in North America and Britain. Nat Med. 1995;1(7):661-6.
34. Berry JL, Pelicic V. Exceptionally widespread nanomachines composed of type IV pilins: the prokaryotic Swiss Army knives. FEMS Microbiol Rev. 2015;39(1):134-54.
35. Urban TA, Griffith A, Torok AM, Smolkin ME, Burns JL, Goldberg JB. Contribution of Burkholderia cenocepacia flagella to infectivity and inflammation. Infect Immun. 2004;72(9):5126-34.
36. Hayashi F, Smith KD, Ozinsky A, Hawn TR, Yi EC, Goodlett DR, et al. The innate immune response to bacterial flagellin is mediated by Toll-like receptor 5. Nature. 2001;410(6832):1099-103.
37. Coenye T, Van Acker H, Peeters E, Sass A, Buroni S, Riccardi G, et al. Molecular mechanisms of chlorhexidine tolerance in Burkholderia cenocepacia biofilms. Antimicrob Agents Chemother. 2011;55(5):1912-9.

38. Nair BM, Cheung KJ Jr, Griffith A, Burns JL. Salicylate induces an antibiotic efflux pump in Burkholderia cepacia complex genomovar III (B. cenocepacia). J Clin Invest. 2004;113(3):464-73.
39. Corral J, Perez-Varela M, Barbe J, Aranda J. Direct interaction between RecA and a CheW-like protein is required for surface-associated motility, chemotaxis and the full virulence of Acinetobacter baumannii strain ATCC 17978. Virulence. 2020;11(1):315-26.
40. Harding CM, Hennon SW, Feldman MF. Uncovering the mechanisms of Acinetobacter baumannii virulence. Nat Rev Microbiol. 2018;16(2):91-102.
41. Zhang MF, Wan SC, Chen WB, Wang YX, Wang H, Li YQ, et al. Transcription factor Dmrt1 triggers the SPRY1-NF-κB pathway to maintain testicular immune homeostasis and male fertility. Zool Res. 2023;44(3):505-21.
42. Song TZ, Zheng HY, Han JB, Feng XL, Liu FL, Yang X, et al. Northern pig-tailed macaques (Macaca leonina) infected with SARS-CoV-2 show rapid viral clearance and persistent immune response. Zool Res. 2021;42(3):350-3.
43. Uddin TM, Chakraborty AJ, Khusro A, Zidan BRM, Mitra S, Emran TB, et al. Antibiotic resistance in microbes: history, mechanisms, therapeutic strategies and future prospects. J Infect Public Health. 2021;14(12):1750-66.
44. Coates AR, Hu Y. Novel approaches to developing new antibiotics for bacterial infections. Br J Pharmacol. 2007;152(8):1147-54.
45. Ezzeddine Z, Ghssein G. Towards new antibiotics classes targeting bacterial metallophores. Microb Pathog. 2023;182:106221.
46. Xiao YH. Bacterial resistance: challenge and strategies. China Licensed Pharmacist. 2011;8(6):3-8.